

Freak wave prediction from spectra

Nobuhito Mori

Graduate School of Engineering, Osaka City University

Peter A.E.M. Janssen

European Centre for Medium-Range Weather Forecasts

Miguel Onorato

Dip. di Fisica Generale, Università di Torino

1 Introduction

Stories of monstrous waves have been told by sailors (Draper, 1965). For example, the captain of cargo vessel Junior reported a wave estimated to be 100 feet high and the famous reliable report was that of the wave encountered by U.S.S. Ramapo in the North Pacific in 1933; that wave was estimated to be 112 feet high. There are many more reports of encountering similar waves in the history of the seas. Evidence of these extreme waves has become increasingly substantial during the last decade, mainly because of the increase in the number of measurement locations and the increased accuracy of field observations. Also, while in the past quality control was so strict that freak waves were regarded as an outlier and therefore their observation was ignored in the official records, nowadays a more relaxed quality control procedure is followed. Klinting and Sand (1987) reported several extreme wave events, called *freak waves*, recorded in the North Sea. More evidence of freak wave generation in the real ocean was found by analyzing field data of the North Sea (Stansell et al., 2003; Guedes Soares et al., 2003), the Sea of Japan (Yasuda and Mori, 1997; Yasuda et al., 1997) and the Gulf of Mexico (Guedes Soares et al., 2004).

Klinting and Sand (1987) introduced a definition of a freak wave that consists of three rules: .

1. It has a wave height higher than twice the significant wave height.
2. Its wave height is larger than 2 times of the fore-going and the following wave heights.
3. Its wave crest height is larger than 65% of its wave height.

In the course of time the above three conditions have been relaxed into only the first condition and it is this condition that is generally used as a freak wave definition (Sand et al., 1990).

There are two essential arguments for freak wave research. The first important thing is understanding the freak wave generation mechanisms. The above mentioned definition of freak wave is fairly general, therefore, there are several mechanisms to explain why extreme wave events have occurred at sea.

The second aspect of the problem is to establish a reliable statistical model for freak wave occurrence, e.g. which aspects of freak waves can be predicted. A freak wave is one or a few large waves in a wave train and therefore it includes huge statistical sensitivity from mathematical point of view. Moreover, the life of such extreme wave is a transient and the life time of such event may be fairly short. Therefore, the specific freak wave population should be clarified rather than chasing individual wave profiles, although no doubt we learn from observing these individual waves. For given population of freak waves, it is possible to estimate how often waves of any given size will occur.

In the last decades a lot of effort in the oceanographic community has been dedicated to the study of extreme events in the ocean. Nowadays, it is accepted that at least four mechanisms are responsible for the formation of extreme waves. The first one is just linear superposition of waves; in this case the wave height probability distribution obeys, in the limit of the narrow-band approximation, a Rayleigh distribution (Longuet-Higgins, 1952); corrections due to finite spectral band width have been obtained (Næss, 1985; Boccotti, 1989; Tayfun, 1981). Wave crest statistics can be determined by using the second order theory developed by Longuet-Higgins (1963). In the narrow-band approximation, the probability distribution for wave crests has been found in Tayfun (1980) (for finite band-width see Fedele and Arena (2005)). The second mechanism is the interaction of waves with currents. The third mechanism, the one that will be mainly discussed here, concerns the generation of extreme events as a result of the modulational instability, *i.e.* a four wave quasi-resonant interaction process (*e.g.* Yasuda et al., 1992; Yasuda and Mori, 1994; Onorato et al., 2001; Janssen, 2003). This mechanism becomes relevant for long crested waves; in the case of waves with directional spreading it is still not clear what is the role of the modulational instability and consequent formation of extreme events. Numerical results in the freely decaying case (Onorato et al., 2002; Socquet-Juglard et al., 2005) have shown that the addition of finite directional spreading decreases the probability of formation of extreme waves, leading to wave crests distributed according to the Tayfun distribution (Socquet-Juglard et al., 2005). The fourth mechanism is related to crossing-sea states, *i.e.* two sea-systems, for example a swell and a wind sea, with different directions that coexists in some region of the ocean.

In the present paper we will make a detailed comparison between experimental data from the Marintek wave tank facility, observed data and theory in Mori and Janssen (2006) of a number of statistical parameters, namely, the kurtosis evolution owing to the four wave interactions, the wave height distribution and the maximum wave height distribution. The paper is organized as follows: in section 2 a summary of the results derived in Mori and Janssen (2006) is given, in section 3 the experiments and field observations are described, the comparison of experimental, field data and theory is reported in section 4. The results give a universal theory of extreme wave generation as a consequence of four wave interactions in a unidirectional wave train.

2 Theoretical Background

2.1 Quasi-resonant four wave interactions and high-order moments

As previously mentioned, the modulational instability is a quasi-resonant interaction process, *i.e.* wave numbers and frequencies satisfy the following conditions:

$$\vec{k}_1 + \vec{k}_2 - \vec{k}_3 - \vec{k}_4 = 0 \quad \text{and} \quad \omega(\vec{k}_1) + \omega(\vec{k}_2) - \omega(\vec{k}_3) - \omega(\vec{k}_4) \leq \epsilon^2, \quad (1)$$

here ϵ is a small parameter which corresponds to the steepness in deep water waves. More in particular, the modulational instability takes place when two wave numbers are the same $\vec{k}_1 = \vec{k}_2$ and \vec{k}_3 and \vec{k}_4 are two side bands separated from \vec{k}_1 by Δk , which should be small in order to satisfy the condition (1). The standard kinetic equation that describes the evolution of the wave spectrum in time, Hasselmann (1962), is formally only valid for large times, $O(\epsilon^{-4}\omega_0^{-1})$, and for exact resonances; its extension to quasi-resonant interactions has been obtained in Janssen (2003) where a kinetic equation, which should be also valid on the time scale of the modulational instability, has been derived (see also Annakov and Shrira, 2006). If one then considers the evolution of higher order moments such as the kurtosis, it turns out that the quasi-resonant interactions are responsible for deviations from Gaussian values. In Janssen (2003) the explicit relation between nonlinear interactions of free waves and the fourth order moment of the surface elevation $\eta(\vec{x}, t)$ in deep-water has been investigated. The result is

$$\begin{aligned} \kappa_{40} &= \frac{\langle \eta^4 \rangle}{m_0^2} - 3 \\ &= \frac{12}{g^2 m_0^2} \int d\vec{k}_{1,2,3,4} T_{1,2,3,4} \sqrt{\omega_1 \omega_2 \omega_3 \omega_4} \delta_{1+2-3-4} R_r(\Delta\omega, t) N_1 N_2 N_3 \end{aligned} \quad (2)$$

where m_0 is the variance of the surface elevation η , κ_{40} is the fourth order cumulant of the surface elevation (equals to kurtosis minus 3), g is the acceleration of gravity, k is the wave number, ω is the angular frequency, N is the wave action spectral density, $T_{1,2,3,4}$ is the coupling coefficient in the Zakharov equation (see Krasitskii (1994) for its analytical form), $\delta_{1+2-3-4} = \delta(\vec{k}_1 + \vec{k}_2 - \vec{k}_3 - \vec{k}_4)$, $d\vec{k}_{1,2,3,4} = d\vec{k}_1 d\vec{k}_2 d\vec{k}_3 d\vec{k}_4$ and $R_r = (1 - \cos(\Delta\omega t))/\Delta\omega$ is the resonance function. In the limit of large times $R_r \rightarrow \mathcal{P}/\Delta\omega$, where $\Delta\omega = \omega_1 + \omega_2 - \omega_3 - \omega_4$ and \mathcal{P} denotes the principle value of the integral to avoid singularity in the integral.

In the narrow-band approximation, assuming that the spectrum $E(\omega)$ has a Gaussian shape:

$$E(\omega) = \frac{m_0}{\sigma_\omega \sqrt{2\pi}} e^{-\frac{1}{2}\nu^2}, \quad (3)$$

where $\nu = (\omega - \omega_0)/\sigma_\omega$ and σ_ω is the spectral band-width, the integral in (2) for large times becomes:

$$\kappa_{40} = \frac{24\epsilon^2}{\Delta^2} \mathcal{P} \int \frac{d\nu_{1,2,3}}{(2\pi)^{3/2}} \frac{e^{-\frac{1}{2}[\nu_1^2 + \nu_2^2 + \nu_3^2]}}{(\nu_1 + \nu_2 - \nu_3)^2 - \nu_1^2 - \nu_2^2 + \nu_3^2}, \quad (4)$$

where $\epsilon = k_0 \sqrt{m_0}$ is the steepness parameter and $\Delta = \sigma_\omega/\omega_0$ is the relative spectral band-width. The integral can be evaluated analytically to obtain:

$$\kappa_{40} = \frac{\pi}{\sqrt{3}} BFI^2 \quad (5)$$

where BFI is defined as in Janssen (2003)

$$BFI = \frac{\epsilon}{\Delta} \sqrt{2}. \quad (6)$$

Eq. (5) is the simplified prediction equation of the kurtosis of the surface elevation assuming a narrow-band, unidirectional wave train, but the full description requires the evaluation of a six dimensional integral in wave number space, Eq. (2).

2.2 Wave height and maximum wave height distribution

In order to include nonlinear effects in the wave height distribution function giving possible deviations from the Rayleigh statistics, the standard approach is to use the Edgeworth series developed at the beginning of the last century (*e.g.* Edgeworth, 1907). The theory for wave height is described in Tayfun and Lo (1990); Mori and Yasuda (2002); Mori and Janssen (2006). The resulting distribution has been named the Modified Edgeworth Rayleigh (MER) distribution. The MER wave height and exceedance wave height distribution are given by Mori and Janssen (2006):

$$p(H)dH = \frac{1}{4} H e^{-\frac{1}{8}H^2} [1 + \kappa_{40} A_H(H)] dH, \quad (7)$$

$$P_H(H) = e^{-\frac{1}{8}H^2} [1 + \kappa_{40} B_H(H)], \quad (8)$$

where H is the wave height normalized by $\eta_{rms} = \sqrt{m_0}$, κ_{40} is defined in Eq. (4) and $A_H(H)$ and $B_H(H)$ are polynomials defined as

$$A_H(H) = \frac{1}{384} (H^4 - 32H^2 + 128), \quad (9)$$

$$B_H(H) = \frac{1}{384} H^2 (H^2 - 16). \quad (10)$$

Note that these distributions describe the deviation from linear statistics under the hypothesis of a narrow-band, weakly nonlinear wave train. Second order contributions, which are important for the distribution of wave crests, can be included by using a Tayfun-like approach (Tayfun, 1980) (see also Tayfun (2006)).

Using Eqns. (7-8) the probability distribution function p_m and the exceedance probability P_m of maximum wave height can be given as a function of the fourth cumulant of the surface elevation κ_{40} and the number of waves N recorded in the wave train,

$$p_m(H_{max}) = \frac{N}{4} H_{max} e^{-\frac{H_{max}^2}{8}} [1 + \kappa_{40} A_H(H_{max})] \times \exp \left\{ -N e^{-\frac{H_{max}^2}{8}} [1 + \kappa_{40} B_H(H_{max})] \right\}, \quad (11)$$

$$P_m(H_{max}) = 1 - \exp \left\{ -N e^{-\frac{H_{max}^2}{8}} [1 + \kappa_{40} B_H(H_{max})] \right\}, \quad (12)$$

where H_{max} is the maximum wave height normalized by η_{rms} . In Mori and Janssen (2006) a comparison of the theoretical wave height distribution with field data have shown qualitative agreement. For $\kappa_{40} = 0$, results are identical to the ones following from the Rayleigh distribution.

Note that simpler looking expressions for the wave height and maximum wave height distribution may be obtained by normalizing with the significant wave height $H_s = 4\sqrt{m_0}$. We record these expressions for completeness. Hence, normalizing with the significant wave height, Eq. (7)-Eq. (12) become

$$p^*(H^*)dH^* = 4H^*e^{-2H^{*2}} [1 + \kappa_{40}A_H^*(H^*)] dH^*, \quad (13)$$

$$P_H^*(H^*) = e^{-2H^{*2}} [1 + \kappa_{40}B_H^*(H^*)], \quad (14)$$

$$A_H^*(H^*) = \frac{1}{3} (2H^{*4} - 4H^{*2} + 1), \quad (15)$$

$$B_H^*(H^*) = \frac{2}{3}H^{*2} (H^{*2} - 1). \quad (16)$$

while the maximum wave height distribution and the exceedance probability becomes

$$p_m^*(H_{max}^*) = 4NH_{max}^* e^{-2H_{max}^{*2}} [1 + \kappa_{40}A_H^*(H_{max}^*)] \\ \times \exp \left\{ -Ne^{-2H_{max}^{*2}} [1 + \kappa_{40}B_H^*(H_{max}^*)] \right\}, \quad (17)$$

$$P_m^*(H_{max}^*) = 1 - \exp \left\{ -Ne^{-2H_{max}^{*2}} [1 + \kappa_{40}B_H^*(H_{max}^*)] \right\}. \quad (18)$$

where H_{max}^* is the maximum wave height normalized by H_s .

If one defines a freak wave as a wave whose height $H_{freak} \geq 2H_s$, we obtain from Eq. (12) or Eq. (18) the following simple formula to predict the occurrence probability of a freak wave as function of N and κ_{40} ,

$$P_{freak} = 1 - \exp [-\beta N(1 + 8\kappa_{40})] \quad (19)$$

where $\beta = e^{-8}$ is constant. The term $8\kappa_{40}$ is the nonlinear correction to linear theory for the maximum wave height distribution. Thus, the nonlinear correction to the maximum wave height depends on κ_{40} .

To summarize the above discussion, we can state that the quasi-resonant four wave interactions introduce deviations from linear expectations of the statistics of surface elevation; in particular, for weakly nonlinear, narrow-banded and long-crested wave trains, the kurtosis evolves according to Eq. (2). In the narrow-band approximation, the kurtosis is related to the BFI; the tail of wave height distribution depends on the kurtosis/BFI and increases as the kurtosis increases. Finally, the maximum wave height distribution depends on both the number of waves in the wave train (record length) and the kurtosis, see Eq. (11).

3 Experimental and Field Data

The experiment was carried out in the long wave flume at Marintek; experimental details and some data analysis can be found in Onorato et al. (2006). The length of the tank is 270 m and its width is 10.5 m; the depth is 10 meters for the first 85 meters and 5 meters for the rest of the flume. For the wavelengths considered in the experiments, the deep water conditions apply through the tank. The wave surface elevation was measured simultaneously by 19 probes placed at different locations along the flume. The sampling frequency for each probe was 40 Hz. The capacitance wave gauges were used for the surface displacement measurements. A view of the flume with the location of the probes is shown

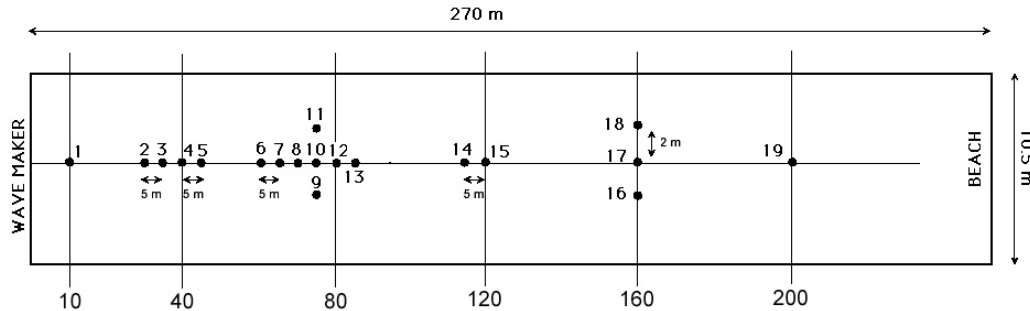


Figure 1: Sketch of the wave tank facility at Marintek and location of wave probes

in Figure 1. JONSWAP random wave signals were generated at the wave maker as sums of independent harmonic components, by means of the inverse Fast Fourier Transform of complex random Fourier amplitudes. These were prepared according to the “random phase approach” by using random Fourier amplitudes as well as random phases. This implies that, due to the central limit theorem, κ_{40} should ideally be equal to zero and μ_4 equal to 3. As mentioned in the previous section, the maximum wave height depends on the number of waves in the wave train in both linear and nonlinear theory as shown in Eq. (11). Hence, the large number of waves is fundamental for the convergence both of the tail of the PDF of wave height and the maximum wave height. Therefore, 5 different realizations with different sets of random phases have been performed. The duration of each realization was 32 minutes. The total number of wave heights (counting both up-crossing and down-crossing) recorded for each spectral shape at each probe was about 12800 waves. This is a sufficient number of waves to check the sensitivity of the maximum wave height distribution on the number of waves. The spatial evolution of wave statistics is described in Onorato et al. (2006).

The field observations were originally collected by the Tokyo Electric Power Company using an ultra sonic wave gauge at a depth of 30m, off the coast of the Pacific Ocean. The length of each record was 20min and the data were collected every hour from March 1 to the end of June in 2001. The wave statistics such as H_{max} , $H_{1/3}$, $T_{1/3}$, N , μ_3 , and μ_4 were operationally calculated and archived. Note that the water depth of 30m is relatively shallow water. Therefore, to eliminate shallow water effects¹, the data are excluded if the dimensionless water depth $k_p h$ is less than 2.0 (it corresponds to $T_{1/3} \geq 8$ s). The total number of valid data was about 2546. The detailed analysis of the data is described in Mori and Janssen (2006).

4 Comparison of observations and theory

The consequences of the maximum wave height distribution (Eq. (11)) are in general hard to verify, not only because Eq. (11) depends on the number of waves considered but also because nonlinear effects are included in the distribution via the kurtosis which requires a large number of data to converge. Nevertheless, the present laboratory data set seems to be

¹in the context of the nonlinear Schrödinger equation there is only nonlinear focusing for $k_p h > 1.36$

suitable for such comparison (as previously described, the time series are very long). Figure 2 shows the comparison of the maximum wave height distribution from observations from the lab and the field with Eq.(11) for $N = 150$. The filled circles \bullet denote the laboratory data, the filled triangle \blacktriangle denote the field data, the maximum wave height distribution from Rayleigh theory (denoted Rayleigh H_{max} distribution hereafter) is represented by the dotted line, while Eq.(12) (denotes MER H_{max} distribution hereafter) corresponds to the solid line. To obtain a distribution of maximum wave height, each laboratory record is divided in smaller time series containing each 150 waves; the maximum wave heights are then collected from the shorter time series. The field data were treated slightly differently: time series were labelled as having a particular N value and μ_4 value when the actual values matched $N \pm 25$ and $\mu_4 \pm 0.1$. There were insufficient number of samples for the larger kurtosis case (Figure 2(c)) In Figure 2 (a) the comparison between theory and experiment is shown for linear wave condition ($\mu_4 = 3$). The peak of the observed maximum wave height distribution is larger than the Rayleigh H_{max} distribution and the MER H_{max} distribution with $\mu_4 = 3.06$ but the observed distribution is more narrow (we ascribe this difference to effects of finite width of the spectrum). As waves propagate through the flume, the nonlinear dynamics results in an increase of the kurtosis and therefore the maximum wave height distribution of the laboratory data departs from the Rayleigh distribution (Figure 2 (a) \rightarrow (c)) and the peak of the observed distribution shift to larger wave heights. While the Rayleigh H_{max} distribution is independent of the kurtosis, the MER H_{max} distribution follows decently the behavior of the experimental data. The MER H_{max} distribution seems to reproduce reasonably well both the laboratory and field data; for very small kurtosis, it overestimates the experimental data and for large kurtosis it slightly underestimates the data.

Here we also discuss the general behavior of the probability density function of maximum wave height in the nonlinear wave field, by plotting the expected value of the maximum wave height, indicated by $\langle \rangle$, as a function of μ_4 and N , see Figure 3. The number of waves in the field data set could not be fixed as in the analysis of the laboratory data, thus field data were classified into each bin of μ_4 and N . In this Figure we show the numerically integrated value of Eq.(11) and the ensemble average of the experimental and field data. The $\langle H_{max}/H_{1/3} \rangle$ according to the Rayleigh theory corresponds to Figure 3 with $\mu_4 = 3$. The dependence of $\langle H_{max}/H_{1/3} \rangle$ on μ_4 and N is clear both from the laboratory and field data and from Eq.(11). Overall, $\langle H_{max}/H_{1/3} \rangle$ of the laboratory data is smaller than the MER H_{max} distribution and $\langle H_{max}/H_{1/3} \rangle$ of the field data is larger than the MER H_{max} distribution. The theoretically predicted $\langle H_{max}/H_{1/3} \rangle$ is overestimated compared to the laboratory data but it agrees with the laboratory data in a qualitative sense. $\langle H_{max}/H_{1/3} \rangle$ from the field data monotonically increases with increasing μ_4 , but for high kurtosis values the theoretically estimated value of $\langle H_{max}/H_{1/3} \rangle$ is lower.

Finally, Figure 4 shows the comparison of freak wave occurrence frequency P_{freak} obtained from the laboratory data and theory. For small kurtosis waves, $\mu_4 < 3.5$, the freak wave occurrence frequency estimated by the MER H_{max} distribution is larger than what is obtained from the laboratory data. However, the laboratory data show a rapid growth of the occurrence probability of freak waves for larger kurtosis, $\mu_4 > 3.5$. This discrepancy between theory and laboratory data is presently not well-understood.

5 Conclusion

In the present paper a detailed comparison between laboratory data, consisting of a large number of waves, field data and the theoretical expectation described in Mori and Janssen (2006) have been discussed. As the kurtosis increases, the probability of large amplitude waves also increases. Comparison of the MER distribution for maximum wave height with laboratory data and field data has shown a much better agreement than when the maximum wave height distribution obtained from Rayleigh distribution is used. Overall, the theory originally described by Edgeworth at the beginning of the last century, combined with four-wave, quasi-resonant interaction theory and wave statistical theory seems to be an interesting approach for predicting extreme waves in long crested conditions. We should emphasize here that the theory does not need any empirical, ad-hoc parameter.

Here, we showed how accurate theoretical freak wave prediction is for given kurtosis value. There is still remaining the prediction of kurtosis from the spectra. In addition, in real sea states directional effects are important. In this paper we have concentrated on the idea of extreme wave generation owing to four wave interactions in a unidirectional wave train. Presently we are extending the theory to including directional wave effects. This will be discussed in near future.

6 Acknowledgments

NM and MO wish to thank the financial support by European Centre for Medium-Range Weather Forecasts during their stay as visiting scientists there. NM also wish to thank the financial support by JSPS. We thank the European Union (contract HPRI-CT-2001-00176) for making the experiments in Marintek possible. C.T. Stansberg and L. Cavaleri are also acknowledged for their valuable help during the experiments.

References

- Annekov, S. and V. Shrira (2006). Role of non-resonant interactions in evolution of nonlinear random water wave fields. *Journal of Fluid Mechanics* 561, 181.
- Boccotti, P. (1989). *On Mechanics of Irregular Gravity Waves*, Chapter VIII, pp. 111–70. Number 19. Atti Accademia Nazionale dei Lincei, Memorie.
- Draper, L. (1965). ‘freak’ ocean waves. *Marine Observer* 35, 193–195.
- Edgeworth, F. (1907). On the representation of statistical frequency by a series. *Journal of the Royal Statistical Society* 70, 102–106.
- Fedele, F. and F. Arena (2005). Weakly nonlinear statistics of high non-linear random waves. *Physics of Fluids* 17, 026601.
- Guedes Soares, G., Z. Cherneva, and E. Antao (2003). Characteristics of abnormal waves in North Sea storm sea steas. *Applied Ocean Research* 25, 337–344.
- Guedes Soares, G., Z. Cherneva, and E. Antao (2004). Abnormal waves during hurricane Camille. *Journal of Geophysical Research, Ocean* 109, C08008.

- Hasselmann, K. (1962). On the nonlinear energy transfer in gravity-wave spectrum. I. General theory. *Journal of Fluid Mechanics* 12, 481–500.
- Janssen, P. (2003). Nonlinear four-wave interactions and freak waves. *Journal Physical Oceanography* 33(4), 863–884.
- Klinting, P. and S. Sand (1987). Analysis of prototype freak waves. In R. Darlymple (Ed.), *Coastal Hydrodynamics*, pp. 618–632. ASCE.
- Krasitskii, V. (1994). On reduced equations in the Hamiltonian theory of weakly nonlinear surface waves. *Journal of Fluid Mechanics* 272, 1–20.
- Longuet-Higgins, M. (1952). On the statistical distribution of the heights of sea waves. *J. Marine Res.* 11, 245–266.
- Longuet-Higgins, M. (1963). The effect of non-linearities on statistical distributions in the theory of sea waves. *Journal of Fluid Mechanics* 17, 459–480.
- Mori, N. and P. Janssen (2006). On kurtosis and occurrence probability of freak waves. *Journal of Physical Oceanography* 36(7), 1471–1483.
- Mori, N. and T. Yasuda (2002). A weakly non-gaussian model of wave height distribution for random wave train. *Ocean Engineering* 29(10), 1219–1231.
- Næss, A. (1985). On the distribution of crest-to-trough wave heights. *Ocean Engineering* 12(3), 221–234.
- Onorato, M., A. Osborne, and M. Serio (2002). Extreme wave events in directional, random oceanic sea states. *Physics of Fluids* 14, L25–L28.
- Onorato, M., A. Osborne, M. Serio, and S. Bertone (2001). Freak waves in random oceanic sea states. *Physical Review Letter* 86(25), 5831–5834.
- Onorato, M., A. Osborne, M. Serio, L. Cavaleri, C. Brandini, and C. Stansberg (2006). Extreme waves, modulational instability and second order theory: wave flume experiments on irregular waves. *European Journal of Mechanics B/Fluids*, in press.
- Sand, S., N. O. Hansen, P. Klinting, O. Gudmestad, and M. Sterndorff (1990). *Freak wave kinematics*, pp. 535–549. Kluwer Academic Pub.
- Socquet-Juglard, H., K. Dysthe, K. Trulsen, K. H.E., and L. J. (2005). Probability distribution of surface gravity waves during spectral changes. *Journal of Fluid Mechanics* 542, 195–216.
- Stansell, P., J. Wolfram, and S. Zachary (2003). Horizontal asymmetry and steepness distributions for wind-driven ocean waves. *Appl. Ocean Research*, 25, 137–155.
- Tayfun, M. (1980). Narrow band nonlinear sea waves. *Journal of Geophysical Research, Ocean* 85(C3), 1548–1552.
- Tayfun, M. (1981). Distribution of crest-to-trough wave heights. *Journal of Waterway, Port, Coastal and Ocean Engineering*, 149–158.

- Tayfun, M. (2006). Statistics of nonlinear wave crests and groups. *Ocean Engineering* 33(11-12), 589–1622.
- Tayfun, M. and J.-M. Lo (1990). Nonlinear effects on wave envelope and phase. *Journal of Waterway, Port, Coastal and Ocean Engineering* 116(1), 79–100.
- Yasuda, T. and N. Mori (1994). High order nonlinear effects on deep-water random wave trains. In *International Symposium: Waves-Physical and Numerical Modelling*, Volume 2, Vancouver, pp. 823–332.
- Yasuda, T. and N. Mori (1997). Occurrence properties of giant freak waves the sea area around Japan. *J. Waterway, Port, Coast. and Ocean Eng.* 123(4), 209–213.
- Yasuda, T., N. Mori, and K. Ito (1992). Freak waves in a unidirectional wave train and their kinematics. In *Proc. of the 23th Int. Conf. on Coastal Eng.*, Volume 1, Venice, pp. 751–764. ASCE.
- Yasuda, T., N. Mori, and S. Nakayama (1997). Characteristics of giant freak waves observed in the Sea of Japan. In *Waves97*, Virginia, VA, pp. 482–495.

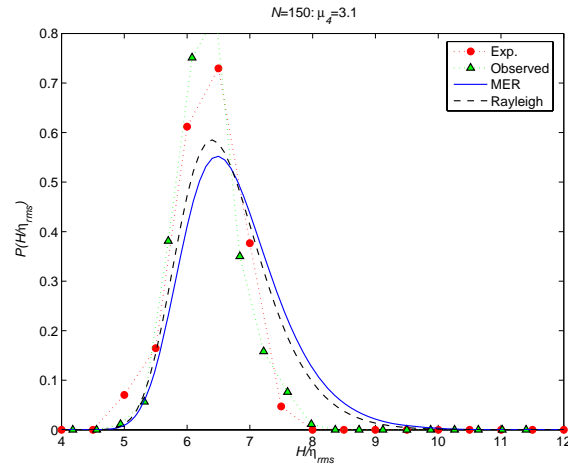
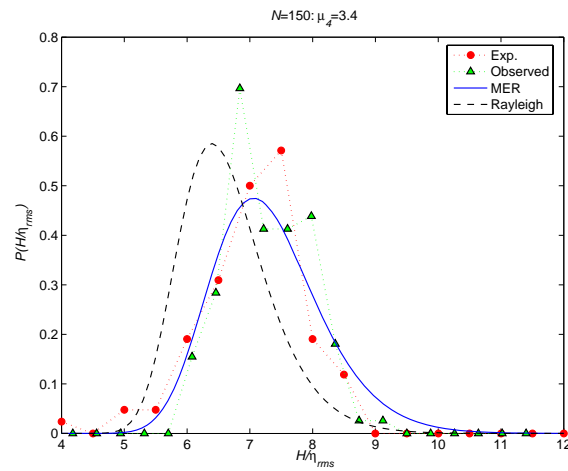
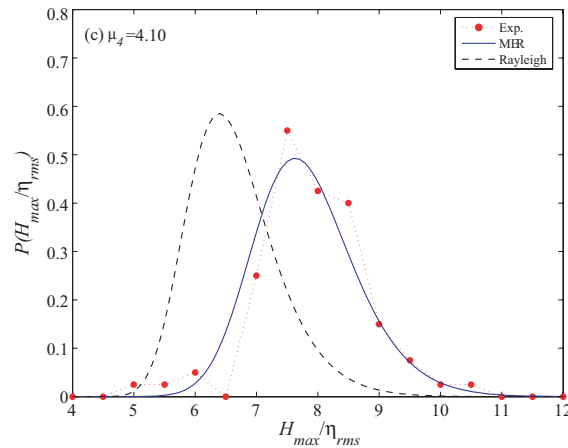
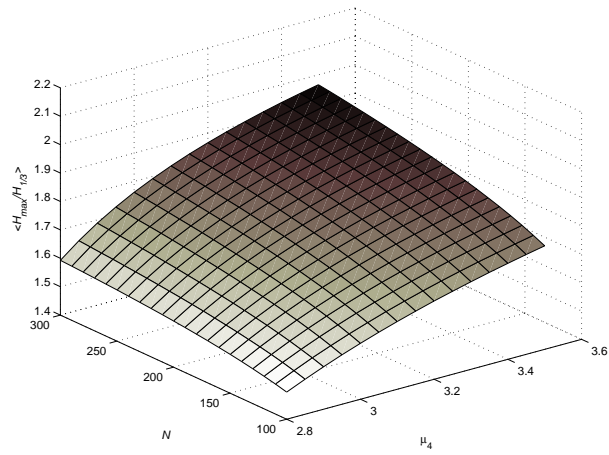
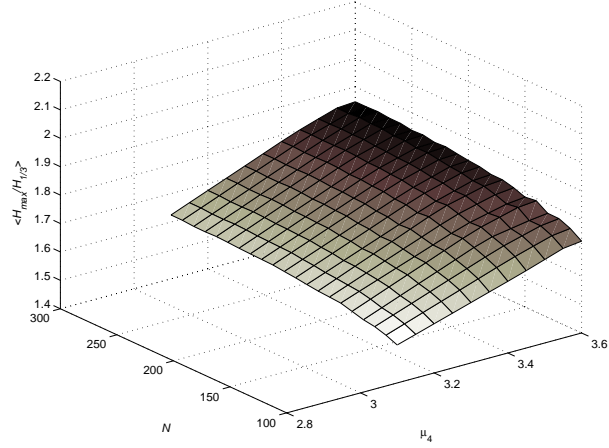
(a) $\mu_4 = 3.06$ (b) $\mu_4 = 3.43$ (c) $\mu_4 = 4.10$

Figure 2: Comparison of maximum wave height distribution H_{max}/η_{rms} with $N = 150$ (\bullet : laboratory data, \blacktriangle : field data, solid line: MER H_{max} distribution, dashed line: Rayleigh H_{max} distribution)

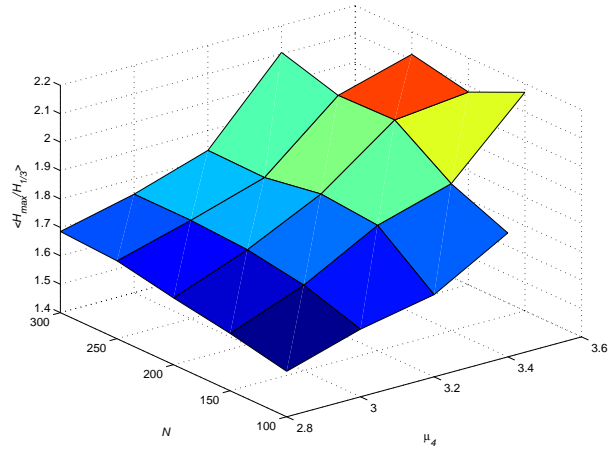


(a) Theory

Experimental data



(b) Laboratory data



(c) Field data

Figure 3: Comparison of $\langle H_{max}/H_{1/3} \rangle$

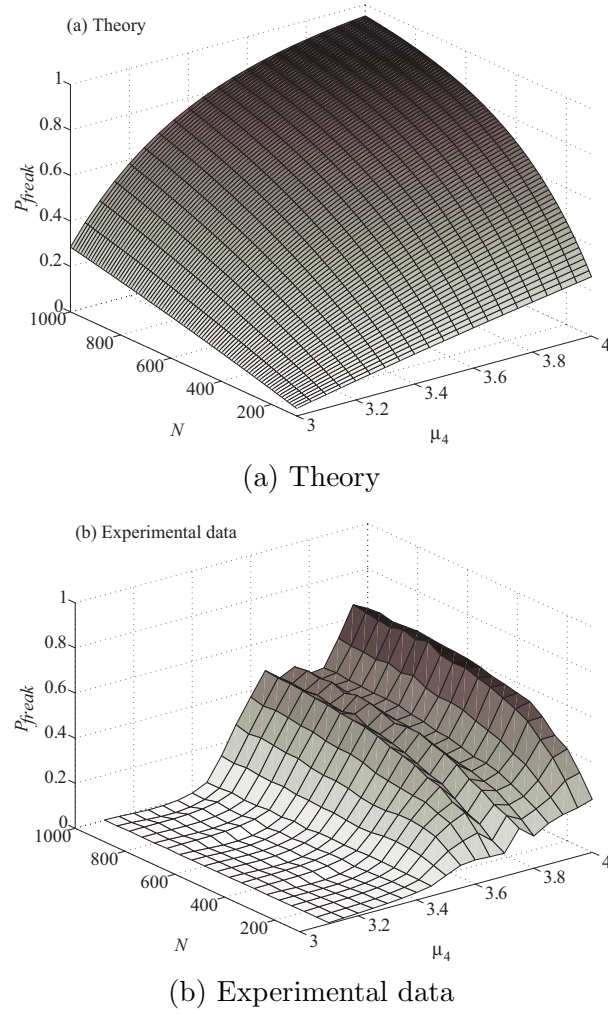


Figure 4: Comparison of occurrence probability of freak wave